

CASZ1 upregulates PI3K-AKT-mTOR signaling and promotes T-cell acute lymphoblastic leukemia

Bruno A. Cardoso,^{1*} Mafalda Duque,^{1*} Ana Gírio,¹ Rita Fragoso,¹ Mariana L. Oliveira,¹ James R. Allen,² Leila R. Martins,¹ Nádia C. Correia,¹ André Bortolini Silveira,³ Alexandra Veloso,² Shunsuke Kimura,⁴ Lisa Demoen,⁵ Filip Matthijssens,⁵ Sima Jeha,^{6,7} Cheng Cheng,⁸ Ching-Hon Pui,^{6,7,9} Ana R. Grosso,^{10,11} João L. Neto,¹ Sérgio F. de Almeida,¹ Pieter Van Vlieberghe,⁵ Charles G. Mullighan,⁴ J. Andres Yunes,³ David M. Langenau,² Françoise Pflumio^{12,13} and João T. Barata¹

¹Instituto de Medicina Molecular João Lobo Antunes, Faculdade de Medicina, Universidade de Lisboa, Lisbon, Portugal; ²MGH Pathology and Harvard Medical School, Charlestown, MA, USA; ³Laboratório de Biologia Molecular, Centro Infantil Boldrini, Campinas, São Paulo, Brazil; ⁴Department of Pathology, Center of Excellence for Leukemia Studies, and Hematological Malignancies Program, St. Jude Children's Research Hospital, Memphis, TN, USA; ⁵Department of Biomolecular Medicine, Ghent University, and Cancer Research Institute Ghent (CRIG), Ghent, Belgium; ⁶Department of Oncology, St. Jude Children's Research Hospital and the University of Tennessee Health Science Center, Memphis, TN, USA; ⁷Department of Global Pediatric Medicine, St. Jude Children's Research Hospital and the University of Tennessee Health Science Center, Memphis, TN, USA; ⁸Department of Biostatistics, St. Jude Children's Research Hospital and the University of Tennessee Health Science Center, Memphis, TN, USA; ⁹Department of Pathology, St. Jude Children's Research Hospital and the University of Tennessee Health Science Center, Memphis, TN, USA; ¹⁰Associate Laboratory i4HB - Institute for Health and Bioeconomy, NOVA School of Science and Technology, Universidade NOVA de Lisboa, Caparica, Portugal; ¹¹UCIBIO - Applied Molecular Biosciences Unit, Department of Life Sciences, NOVA School of Science and Technology, Universidade NOVA de Lisboa, Caparica, Portugal; ¹²Université Paris-Saclay, INSERM, IRCM/IBFJ CEA, UMR Stabilité Génétique Cellules Souches et Radiations, Fontenay-aux-Roses, France and ¹³OPALE Carnot Institute, the Organization for Partnerships in Leukemia, Saint-Louis Hospital, Paris, France

*BAC and MD contributed equally as first authors.

Correspondence: J.T. Barata
joao_barata@medicina.ulisboa.pt

Received: February 10, 2023.
Accepted: November 27, 2023.
Early view: December 7, 2023.

<https://doi.org/10.3324/haematol.2023.282854>

©2024 Ferrata Storti Foundation
Published under a CC BY-NC license



**CASZ1 upregulates PI3K-AKT-mTOR signaling
and promotes T-cell acute lymphoblastic leukemia**

Bruno A. Cardoso*, Mafalda Duque*, Ana Gírio, Rita Fragoso, Mariana L. Oliveira, James R. Allen, Leila R. Martins, Nádia C. Correia, André Bortolini Silveira, Alexandra Veloso, Shunsuke Kimura, Lisa Demoen, Filip Matthijssens, Sima Jeha, Cheng Cheng, Ching-Hon Pui, Ana R. Grosso, João L. Neto, Sérgio F. de Almeida, Pieter Van Vlieberghe, Charles G. Mullighan, J. Andres Yunes, David M. Langenau, Françoise Pflumio and João T. Barata

* These authors contributed equally to this work

SUPPLEMENTARY METHODS

SUPPLEMENTARY REFERENCES

SUPPLEMENTARY FIGURES 1-16

SUPPLEMENTARY TABLE 1

LEGEND TO SUPPLEMENTARY TABLE 2

SUPPLEMENTARY METHODS

Plasmid generation. The pMT2 plasmid was kindly provided by Dr. Paul J. Coffey. The TAL1 coding fragment was amplified by PCR from a pcDNA3.1(+) zeo TAL1 plasmid and inserted in the pMT2 plasmid. The #304-Ø and #304-TAL1 plasmids were generated from the #304.pCCL.sin.cPPT.pA.CTE.eGFP.minCMV.hPGK.deltaNGFR.WPRE (herein called #304-eGFP-deltaNGFR) (1), kindly provided by Dr. Luigi Naldini. Briefly, the #304-eGFP-deltaNGFR plasmid was digested to remove the deltaNGFR fragment and religated creating the #304-Ø vector. To create the #304-TAL1 plasmid, the TAL1 coding fragment (from the pcDNA3.1(+) zeo TAL1 plasmid) was inserted downstream of the hPGK promoter sequence, after removal of the deltaNGFR fragment. The pHR-SIN vectors were previously described (2) and were kindly provided by Dr. Maria L. Toribio. The *CASZ1b* coding fragment was obtained from pCMV-FLAG-CASZ1b (kindly provided by Dr. Carol Thiele) and cloned into pMSCV-IRES-mRFP. The IRES-mRFP and CASZ1b-IRES-mRFP fragments were removed and inserted into the pHR-SIN backbone vector creating the pHR-SIN-mRFP and pHR-SIN-CASZ1b-mRFP plasmids, respectively. The plasmids used to generate transgenic zebrafish have been previously described and included *rag2:mCherry* (3), *rag2:AmCyan* (4) and *rag2:notch1aICD* (5). *rag2:CASZ1b* was created by PCR amplification of the human *CASZ1b* open reading frame and gateway cloning into the *rag2* promoter destination vector using LR clonase II, according to the manufacturer's protocol (Life Technologies). All the plasmids were confirmed by DNA sequencing and the primers are available upon request.

Electroporation of P12 cells. The P12 cell line was transiently transfected with the pMT2-Ø and pMT2-TAL1 plasmids. A total of 30µg of DNA was added to 10⁷ P12 cells in the appropriate volume of pre-warmed RPMI-10 (without antibiotics). Electroporation was performed using Gene Pulser II in 4 cm-gap cuvettes (Bio-Rad) with 350kV and 750µF parameters. Immediately after electroporation, P12 cells were placed in culture and RNA was extracted 48h later.

Nucleofection of Jurkat cells. Jurkat cells were collected by centrifugation, resuspended at 2.5×10^6 cells with 100 μL of the appropriate Nucleofector™ kit solution V (Amaxa Biosystems) and nucleofected with siRNAs (SMARTpool - Dharmacon) using X-001 program of the Nucleofection Device II (Amaxa Biosystems). After nucleofection, the cells were immediately mixed with 500 μL of prewarmed culture medium and transferred into culture plates. The treated cells were incubated at 37°C for 2 days and then used for downstream applications.

[³H] Thymidine incorporation assays. Nucleofected Jurkat cells were cultured in triplicates in flatbottom 96-well plates in regular cultured conditions. Cells were incubated with [³H] thymidine (1 μCi /well) for 16 h before harvest. DNA synthesis, as measured by [³H] thymidine incorporation, was assessed using a liquid scintillation counter. Average and standard deviation of triplicates were calculated.

Apoptosis detection. When indicated determination of Jurkat cellular viability was performed using an Annexin V-based apoptosis detection kit and the manufacturer's protocol (R&D Systems). Briefly, Jurkat cells were suspended in the appropriate binding buffer, stained with FITC-conjugated Annexin V and 7-AAD at room temperature for 15 minutes, and subsequently analyzed by flow cytometry.

Lentiviral transductions. T-ALL primary cells were transduced with G/IL-7SUx envelope pseudotyped vectors. The *TAL1* short hairpin RNA (shTAL1), whose expression is driven by the H1 promoter, was subcloned in the pTRIP/DU3-MND-GFP vector as previously described (6). The control hairpin sequence (shCTL) targets the human hepatitis B virus. After transduction, the cells were washed and cultured with fresh medium for further analysis. Ba/F3 and T-ALL cell lines were transduced with VSV-G-pseudotyped lentiviruses produced by transient transfection of 293T cells, as described (7). Briefly, 10^6 cells were incubated in 1000 ml of the corresponding lentiviral supernatant with 10 $\mu\text{g}/\text{ml}$ Polybrene (Sigma), centrifuged for 2h at 2300 rpm at 33°C, and then washed and cultured in fresh medium. Ba/F3, DND-41, HPB-ALL, Jurkat and MOLT4 cells were transduced with pHR-SIN-mRFP and pHR-SIN-CASZ1b-mRFP. After expansion, the cells were sorted for high RFP expression and cultured as described above. MOLT4 and HPB-ALL cells were transduced with the #304-Ø/TAL1 and #304-ER-Ø/TAL1 vectors, respectively. After expansion, the cells

were sorted for high GFP expression and cultured as described above. CEM and Jurkat cells were transduced with pLentiCRISPR v2 vectors (GenScript) containing gRNAs (#1 gRNA – CGACGGCCGAAGCGCGCCAUGUUUUAGAGCUAUGCU and #4 gRNA – CCACCAACAAUCGAGUGAAGGUUUUAGAGCUAUGCU) to target the *TALI* locus using the CRISPR/cas9 technology. After transduction, the cells were selected with Puromycin (Sigma) and once the viability reached 90%, individual clones were selected by limiting dilution in 96 well-plates. After 3 weeks of culture, expanded clones were tested individually for the different assays.

***In vivo* subcutaneous mouse model.** Mice were housed and bred in a specific pathogen-free animal facility, treated in accordance with the EU guidelines and approval of the Institutional Ethical Committee. Eight-week-old non-obese diabetic/severe-combined immunodeficiency mice (NOD/SCID) mice were subcutaneously injected in the left flank (dorsal view) with 10^7 Ba/F3-empty cells and in the right flank (dorsal view) with Ba/F3-CASZ1b cells. Mice were weighed regularly and monitored closely for assessment of tumor growth. The tumor burden/growth was determined as previously described (8) and the mice were sacrificed when the tumors in the flank reached 1000 mm^3 . To test the efficacy of NVP-BEZ-235 (dactolisib) *in vivo*, 10^7 Ba/F3- CASZ1b cells were subcutaneously injected in the right flank (dorsal view) of eight-week old NOD.Cg-Prkdcg Il2rg^{tm1Wjl} / SzJ (NSG) mice and monitored as described above. When the tumors reached a median volume of 500 mm^3 the mice were randomized into two groups, to receive daily treatment of 50mg/Kg NVP-BEZ-235 dissolved in 10% NMP and 90% PEG-300 or vehicle by oral gavage for 7 consecutive days. The animals were sacrificed once the vehicle-treated mice reached the humane endpoints, the tumors removed, thoroughly minced and lysed for immunoblot analysis.

Zebrafish T-ALL models. Plasmids were linearized with *NotI* and column purified. Mosaic transgenic zebrafish were generated as previously described (9, 10). 40ng/ μL of *rag2:mCherry* or *rag2:AmCyan* was mixed with 40ng/ μL *rag2:notch1aICD* and/or 40ng/ μL *rag2:hCASZ1b* and micro-injected into one-cell stage Tu/AB-strain embryos. Animals were scored for fluorescent-labeled thymocytes at 21 and 28 days post-fertilization (dpf) and followed every 7 days for disease onset and progression. Leukemic fish were defined by >50% of their body being infiltrated with fluorescent-labeled T-ALL cells as previously described (4, 5). The zebrafish were sacrificed when

moribund and the tumors were harvested for further analysis. All zebrafish experiments were approved according to the iMM-JLA's institutional and Portuguese (DGAV) regulations.

Histological and immunohistochemical analysis. Zebrafish were sacrificed when moribund and leukemias were harvested for further analysis. May-Grünwald Giemsa staining was performed as previously described followed by imaging on the Hamamatsu NanoZoomerSQ (11). Fixed zebrafish heads were embedded in paraffin, step sectioned, and stained with hematoxylin and eosin (H&E), phospho-H3 and TUNEL by the Specialized Histopathology Services at MGH, Boston, USA. Sections were imaged at 400X magnification using an Olympus BX41 compound microscope. The ratio of positively stained cells to total cells was calculated in three separate areas of each head. A square root transformation was applied to each data point to stabilize variance and significance was calculated by Student's t-test.

RNA extraction, cDNA synthesis and quantitative-PCR. RNA was extracted as previously described (7), using the RNeasy Mini Kit, according to the manufacturer's instructions (Qiagen). Up to 1 μ g of total RNA was reverse-transcribed using the Superscript III reverse transcriptase and random hexamers according to the manufacturer's instructions (Thermo Fisher Scientific) to generate complementary DNA (cDNA). The expression of a specific gene was evaluated by quantitative real-time polymerase chain reaction (qPCR) and normalized to *GAPDH*, *18S* or *β -actin* house-keeping genes as indicated. The primers used are described in supplementary table 1, mixed with SYBR green master mix (Applied Biosystems) and the reactions performed in a ViiA7 qPCR instrument (Applied Biosystems). Relative transcript expression was estimated using the ddCt method. Samples were run in triplicate, with error bars representing the SEM of compiled data from all replicates and experimental samples.

RNA sequencing (RNAseq) and data analysis. RNA was extracted from Ba/F3-empty and Ba/F3-CASZ1b cells cultured for 6h in RPMI-10 (without IL3) using the RNeasy Mini Kit (Qiagen). Sequencing was performed after non stranded mRNA library preparation in a BGISEQ-500 sequencer (BGI). RNA-seq data quality was assessed using FastQC (v0.11.5, <https://www.bioinformatics.babraham.ac.uk/projects/fastqc/>). Reads were pseudo-aligned to mouse transcriptome (encode M14) with Kallisto

v0.44.0 (12). Differential expression was assessed using edgeR (v3.20.9) and limma (v3.34.9) R packages (13, 14). Briefly, sample comparison was performed using voom transformed values, linear modeling and moderated T-test as implemented in limma R package, selecting significantly differentially expressed genes with appropriate threshold (adjusted P-values lower than 0.05, and absolute $\log_2FC > 1$). Volcano plot was generated using the ggplot2 package (v3.3.1) in R (v3.4.4). Heatmap of transcriptional differences was generated with R package pheatmap (v1.0.12) with clustering performed with hclust from the R stats package. Data are available at SRA (accession number: PRJNA754041).

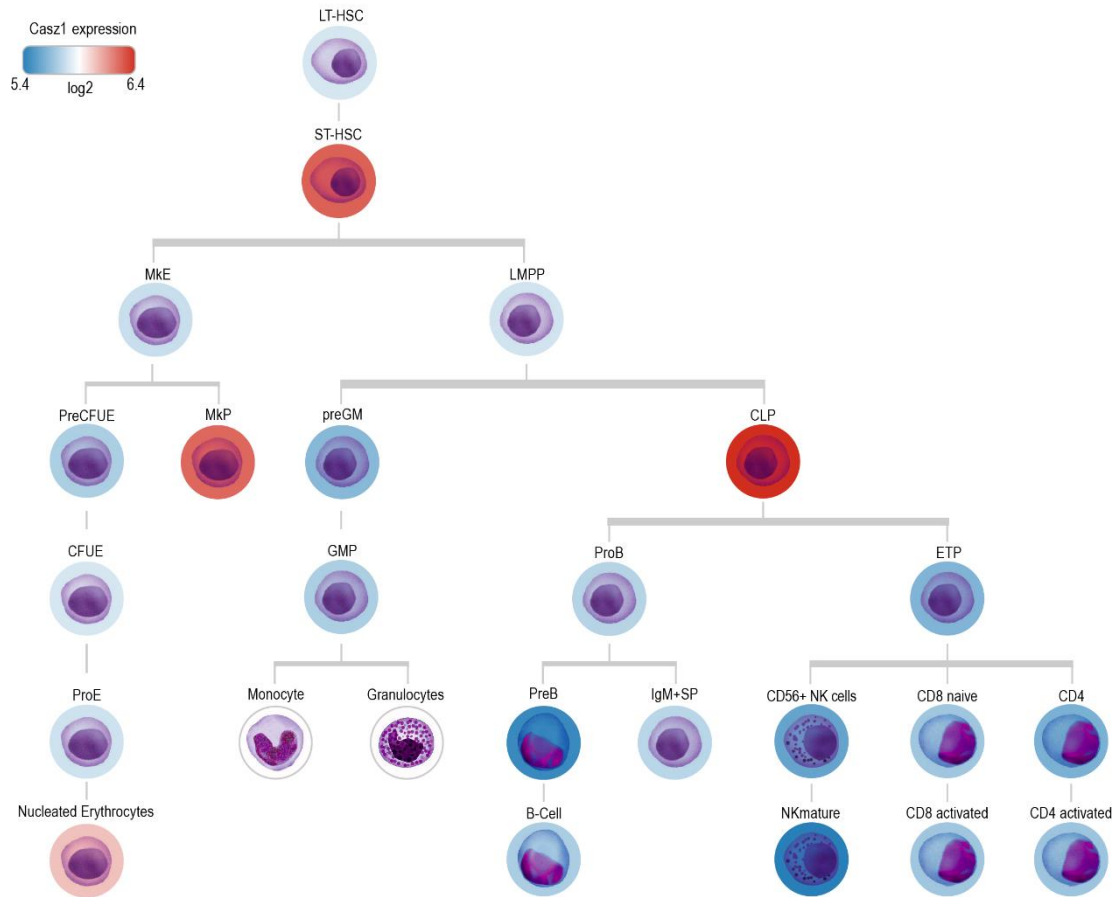
Pathway enrichment analysis. Pathway enrichment analyses were performed using g:profiler's g:GOST functional profiling tool (<https://biit.cs.ut.ee/gprofiler/gost>) against Kyoto Encyclopedia of Genes and Genomes (KEGG) pathways. Significance was set at adj. $p < 0.05$ using the tool's suggested g:SCS multiple comparison correction method. Analyses were performed utilizing significantly upregulated DEGs (adj. $p < 0.05$ and $\log_2FC > 1$) for CASZ1 overexpression in BaF3 cells, and genes highly correlated (Pearson's $r > 0.7$) with CASZ1 expression levels in the T-ALL patient sample cohort. Barplots were generated using the ggplot2 R package.

Gene expression data set analysis. The publicly available database Bloodspot (15) was used to retrieve RNA-seq data during mouse hematopoiesis (https://servers.binf.ku.dk/bloodspot/?gene=CASZ1&dataset=nl_mouse_data - probe 1442010_at). The cell images were adapted from OpenStax Anatomy and Physiology (Version 8.25, <https://openstax.org/books/anatomy-and-physiology/pages/preface>) under the Creative Commons Attribution 4.0 International license. The microarray datasets of T-ALL patients, cell lines and normal controls have been described and are publically available (GEO database, accession number GSE18497, GSE33469, GSE33470, GSE41621, GSE51001 and GSE66638). The expression levels of *CASZ1a*, *CASZ1b* and *TALI* at diagnosis were assessed using the GeoR algorithm and analyzed as described below. T-ALL patients (n=14) from the clinically annotated GSE18497 dataset were divided according to their *CASZ1* transcript levels at diagnosis. Relapse-free and overall survival analyses were performed as described in the Statistical analysis. Using the T-ALL patient samples in the GSE18497 dataset, *CASZ1b* expression at diagnosis was compared and correlated with all the probes in the

microarray. To do this, the probes without any gene and probes with multiple genes attributed were excluded and then Pearson correlation coefficient between the *CASZ1b* probe and all the probes remaining in our analysis was determined. The genes whose correlation coefficient is at least 0.7 (demonstrating a strong positive correlation) were subsequently used to employ KEGG pathway enrichment analysis. RNAseq data of T-ALL patients (n = 153) in St. Jude cohorts (Total 15 and 16) are accessible through St. Jude Cloud at https://platform.stjude.cloud/data/cohorts?dataset_accession=SJC-DS-1009. Both gene- and transcript-level count data were quantitated by RSEM with GRCh38 through STAR mapping. *CASZ1b* count data from transcript-level counts were replaced with gene-level *CASZ1* counts (default was *CASZ1a*), followed by gene expression normalization of gene-level counts by using DEseq2. Survival of patients with high and low *CASZ1b* expression (each 46 cases from top or bottom) were compared and plotted in Kaplan-Meier curves with two-sided log-rank tests. Survival and correlation coefficient analyses were performed using R v.4.2.2 software.

SUPPLEMENTARY REFERENCES

1. Amendola M, Venneri MA, Biffi A, Vigna E, Naldini L. Coordinate dual-gene transgenesis by lentiviral vectors carrying synthetic bidirectional promoters. *Nat Biotechnol.* 2005;23(1):108-116.
2. Zufferey R, Dull T, Mandel RJ, et al. Self-inactivating lentivirus vector for safe and efficient in vivo gene delivery. *J Virol.* 1998;72(12):9873-9880.
3. Smith AC, Raimondi AR, Salthouse CD, et al. High-throughput cell transplantation establishes that tumor-initiating cells are abundant in zebrafish T-cell acute lymphoblastic leukemia. *Blood.* 2010;115(16):3296-3303.
4. Blackburn JS, Liu S, Wilder JL, et al. Clonal evolution enhances leukemia-propagating cell frequency in T cell acute lymphoblastic leukemia through Akt/mTORC1 pathway activation. *Cancer Cell.* 2014;25(3):366-378.
5. Blackburn JS, Liu S, Raiser DM, et al. Notch signaling expands a pre-malignant pool of T-cell acute lymphoblastic leukemia clones without affecting leukemia-propagating cell frequency. *Leukemia.* 2012;26(9):2069-2078.
6. Brunet de la Grange P, Armstrong F, Duval V, et al. Low SCL/TAL1 expression reveals its major role in adult hematopoietic myeloid progenitors and stem cells. *Blood.* 2006;108(9):2998-3004.
7. Cardoso BA, de Almeida SF, Laranjeira AB, et al. TAL1/SCL is downregulated upon histone deacetylase inhibition in T-cell acute lymphoblastic leukemia cells. *Leukemia.* 2011;25(10):1578-1586.
8. Lonetti A, Antunes IL, Chiarini F, et al. Activity of the pan-class I phosphoinositide 3-kinase inhibitor NVP-BKM120 in T-cell acute lymphoblastic leukemia. *Leukemia.* 2014;28(6):1196-1206.
9. Langenau DM, Keefe MD, Storer NY, et al. Co-injection strategies to modify radiation sensitivity and tumor initiation in transgenic Zebrafish. *Oncogene.* 2008;27(30):4242-4248.
10. Oliveira ML, Veloso A, Garcia EG, et al. Mutant IL7R collaborates with MYC to induce T-cell acute lymphoblastic leukemia. *Leukemia.* 2022;36(6):1533-1540.
11. Langenau DM, Traver D, Ferrando AA, et al. Myc-induced T cell leukemia in transgenic zebrafish. *Science.* 2003;299(5608):887-890.
12. Bray NL, Pimentel H, Melsted P, Pachter L. Near-optimal probabilistic RNA-seq quantification. *Nat Biotechnol.* 2016;34(5):525-527.
13. Robinson MD, McCarthy DJ, Smyth GK. edgeR: a Bioconductor package for differential expression analysis of digital gene expression data. *Bioinformatics.* 2010;26(1):139-140.
14. Ritchie ME, Phipson B, Wu D, et al. limma powers differential expression analyses for RNA-sequencing and microarray studies. *Nucleic Acids Res.* 2015;43(7):e47.
15. Bagger FO, Sasivarevic D, Sohi SH, et al. BloodSpot: a database of gene expression profiles and transcriptional programs for healthy and malignant haematopoiesis. *Nucleic Acids Res.* 2016;44(D1):D917-D924.



Supplementary Figure 1. *Cas1* expression is downregulated upon commitment to the T-cell lineage. The *Cas1* transcript levels (RNA-seq data) during mouse hematopoietic differentiation were obtained from the publicly available Bloodspot database.

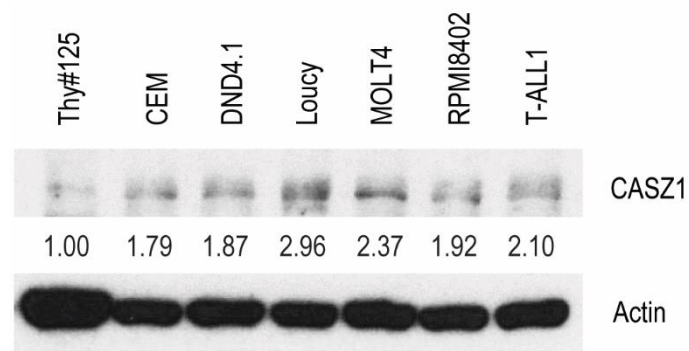
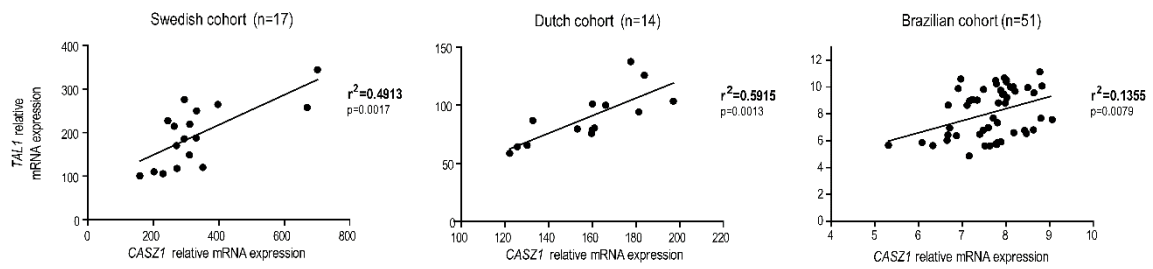
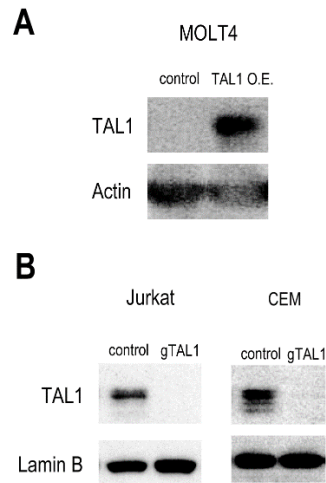


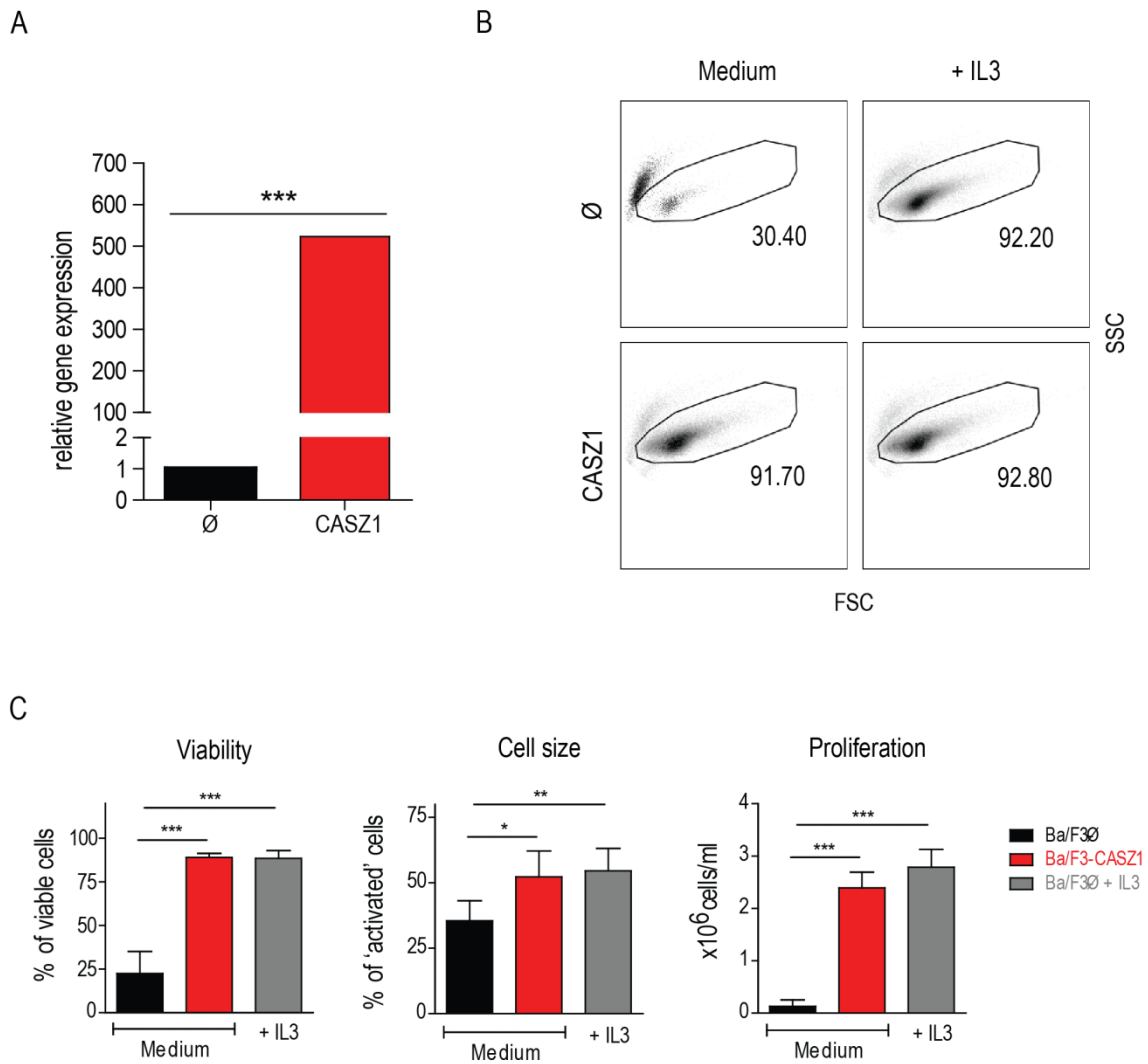
Figure 2. CASZ1 expression is increased in T-ALL cell lines. Cell lysates of normal human thymocytes (Thy#125) and T-ALL cell lines (CEM, DND4.1, Loucy, MOLT4, RPMI8402 and T-ALL1) were analyzed by immunoblotting for the expression of CASZ1. Actin was used as loading control. CASZ1 levels were measured by densitometry analysis, normalized to actin levels and normalized again to the control condition (Thy#125).



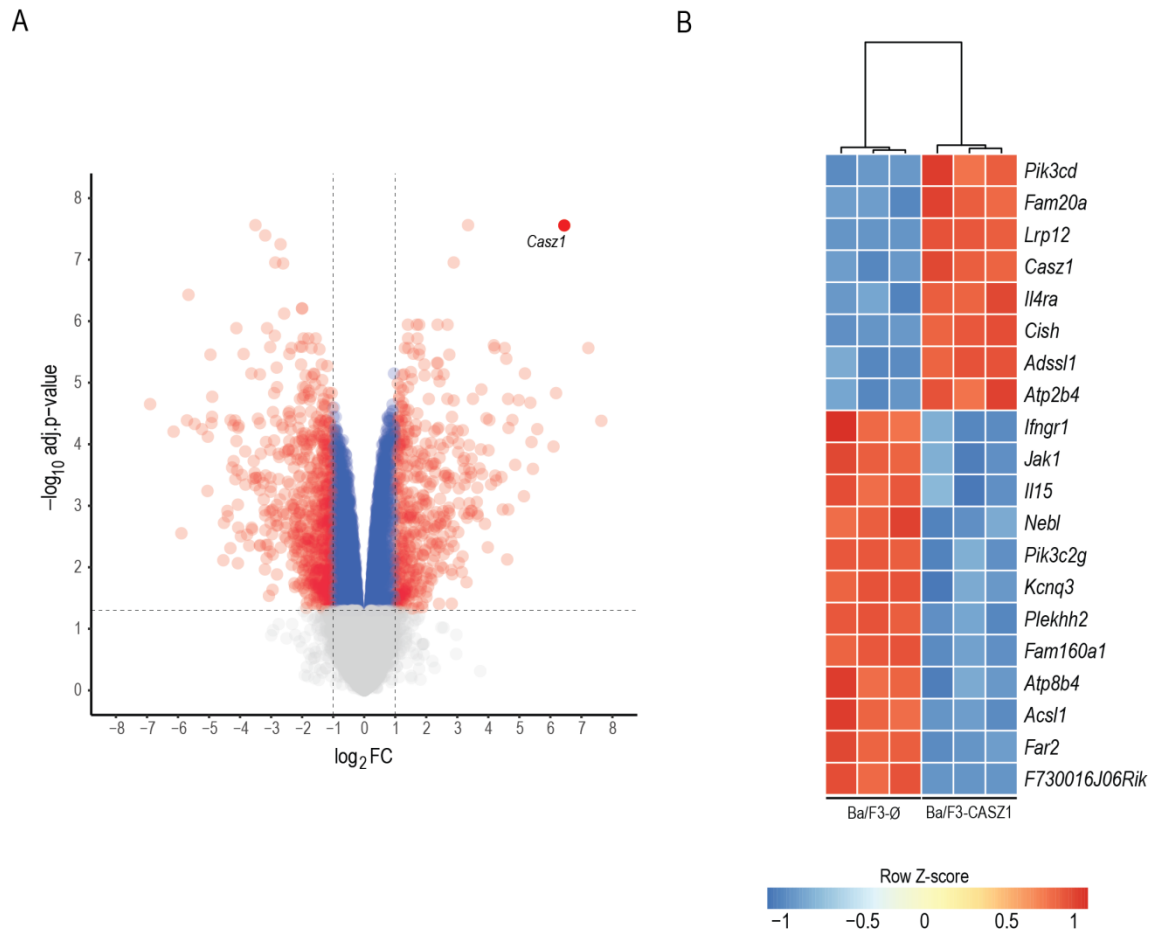
Supplementary Figure 3. CASZ1 mRNA expression at diagnosis correlates with TAL1 mRNA expression. Pearson correlation between *CASZ1b* and *TAL1* transcript levels (log₂ scale) and in three different T-ALL patients cohorts (Swedish - GSE41621, Dutch - GSE18497 and Brazilian - GSE50999 (n=43) and GSE66638 (n=8)). The datasets are publicly available and transcript levels were determined as described in the material and methods section.



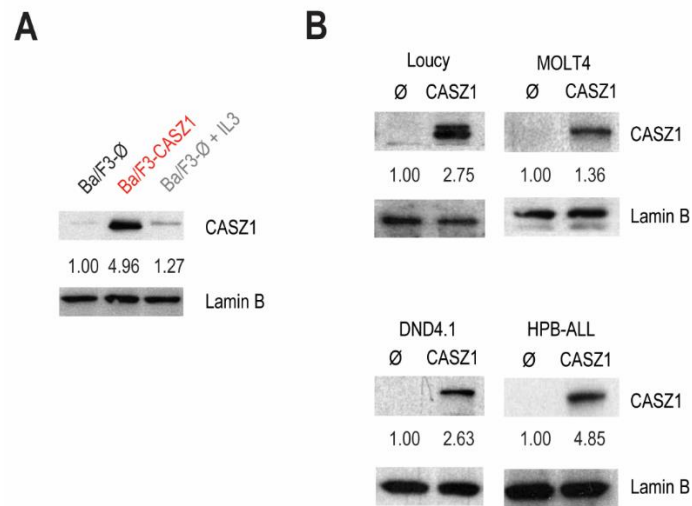
Supplementary Figure 4. Modulation of TAL1 expression in T-ALL cell lines. (A) MOLT4 cells were transduced with the #304-Ø/TAL1 vectors for overexpression of TAL1 protein. Upon transduction, transduced cells were expanded and sorted for GFP expression, lysed and analyzed by immunoblot for TAL1 protein expression. β -Actin protein was used as loading control. Data are representative of two independent experiments. **(B)** Jurkat and CEM cells were transduced with pLentiCRISPR v2 based vectors to target the *TALI* locus using the CRISPR/cas9 technology as described in the methods. The resulting clones were amplified, lysed and analyzed by immunoblot for TAL1 protein expression. Lamin B was used as loading control. Data are representative of three independent established clones.



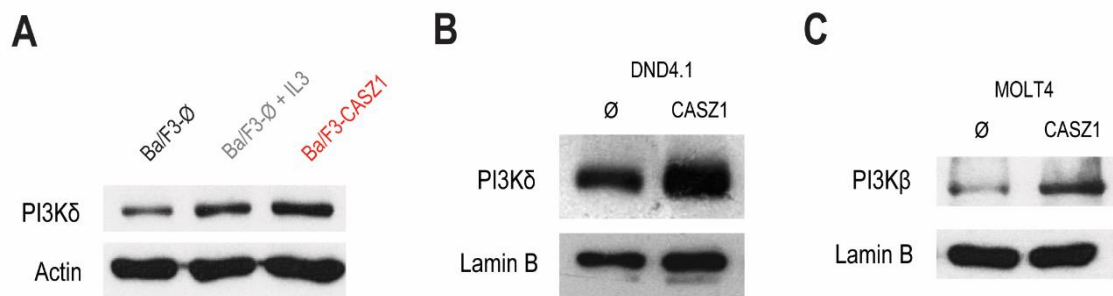
Supplementary Figure 5. CASZ1 overexpression increases viability, cell size and proliferation in Ba/F3 cells. (A) Ba/F3 cells stably expressing *CASZ1b* (CASZ1) or mock vector (Ø) were evaluated for *CASZ1* mRNA levels, determined by qPCR and normalized to the transcript levels of the *18S* house-keeping gene. (B-C) Ba/F3-Ø and Ba/F3-CASZ1 cells were cultured under the indicated conditions for 96h. Viability, cell size and proliferation were determined as described in the methods. (B) Representative dot-plots of at least four independent experiments. (A, C) Values represent the mean \pm standard deviation of at least four experiments. * $p < 0.05$; ** $p < 0.01$; *** $p < 0.001$, one-way analysis of variance.



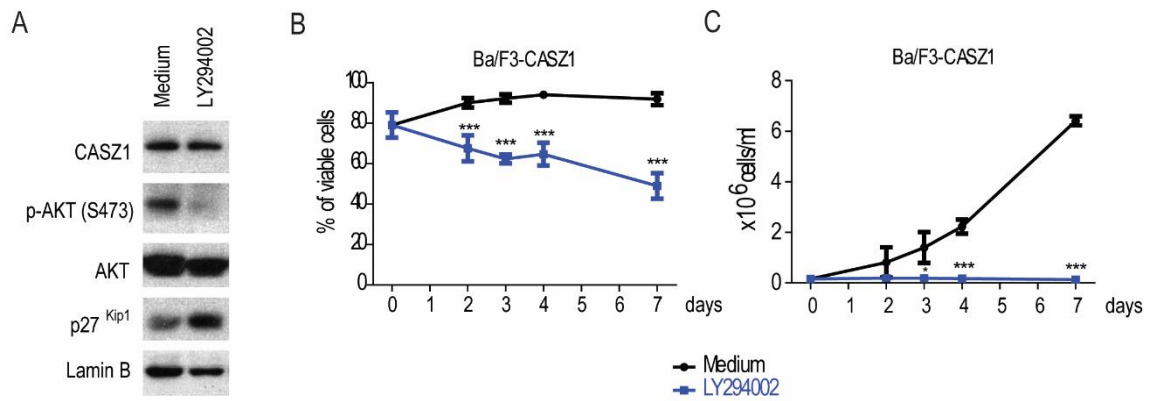
Supplementary Figure 6. CASZ1 overexpression alters the transcriptional program in Ba/F3 cells. (A) Volcano plot of differentially expressed genes of Ba/F3-CASZ1 versus Ba/F3-Ø cells. **(B)** Heat map showing the top 20 differentially expressed genes (DEGs) between the two conditions. The color code reflects the level of expression of the indicated genes.



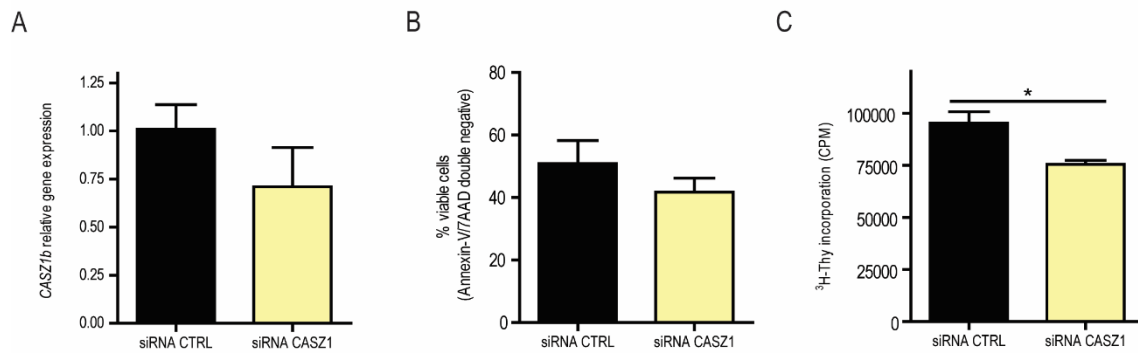
Supplementary Figure 7. CASZ1 protein quantification in immunoblots from figures 3D and 4B. See legend for these figures for sample conditions. CASZ1 levels were measured by densitometry analysis, normalized to Lamin B levels and normalized again to the control conditions (Ø – empty cell lines).



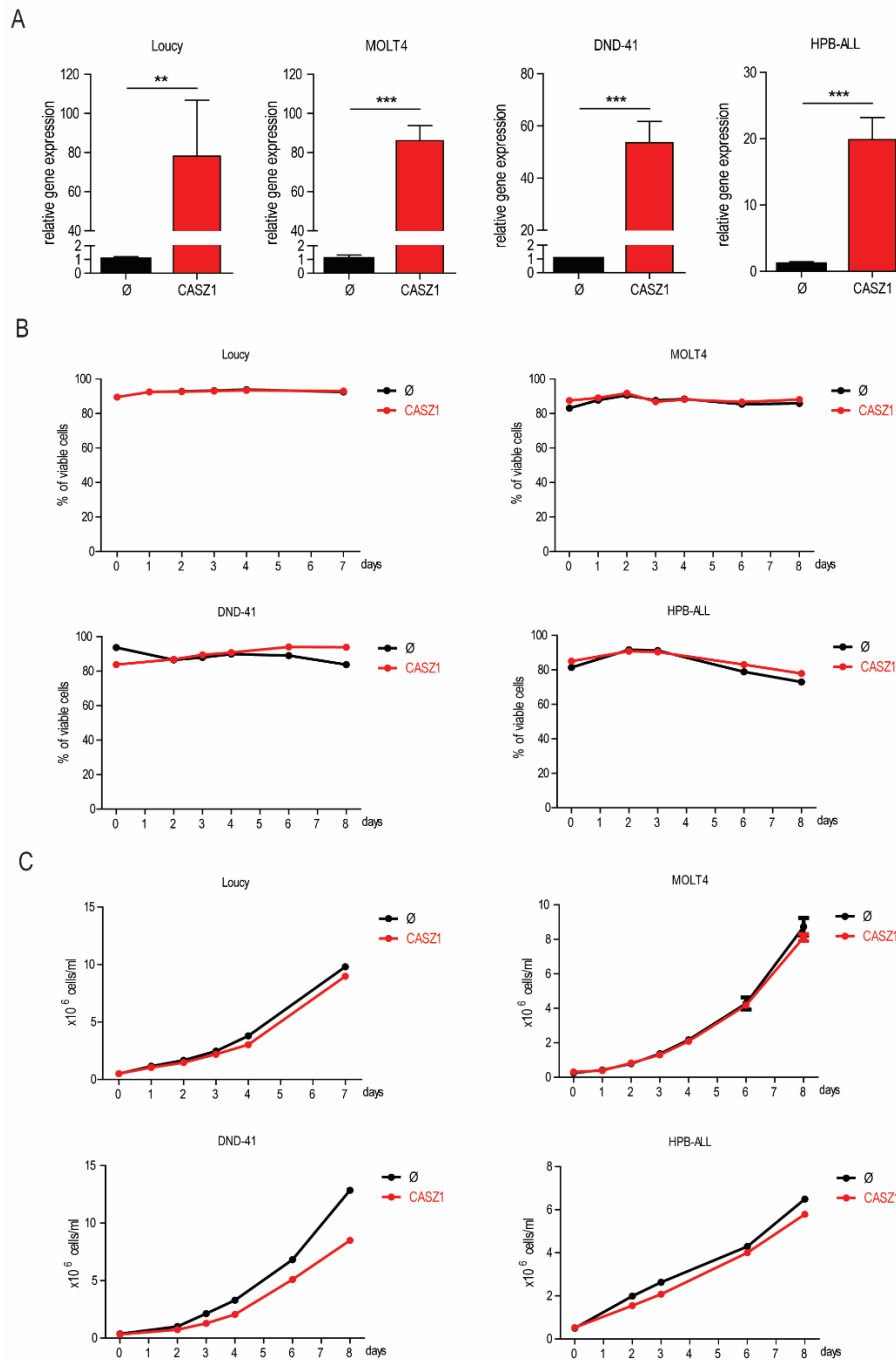
Supplementary Figure 8. CASZ1 expression increases PI3K δ and PI3K β expression. A) Ba/F3- \emptyset and Ba/F3-CASZ1 cells were cultured in the indicated conditions for 24h and PI3K δ expression was evaluated by immunoblot. Actin was used as loading control. B-C) DND4.1- and MOLT4- \emptyset and -CASZ1 expressing cells were analyzed for PI3K δ (B) and PI3K β expression. Lamin B was used as a loading control. Data is representative of two independent experiments.



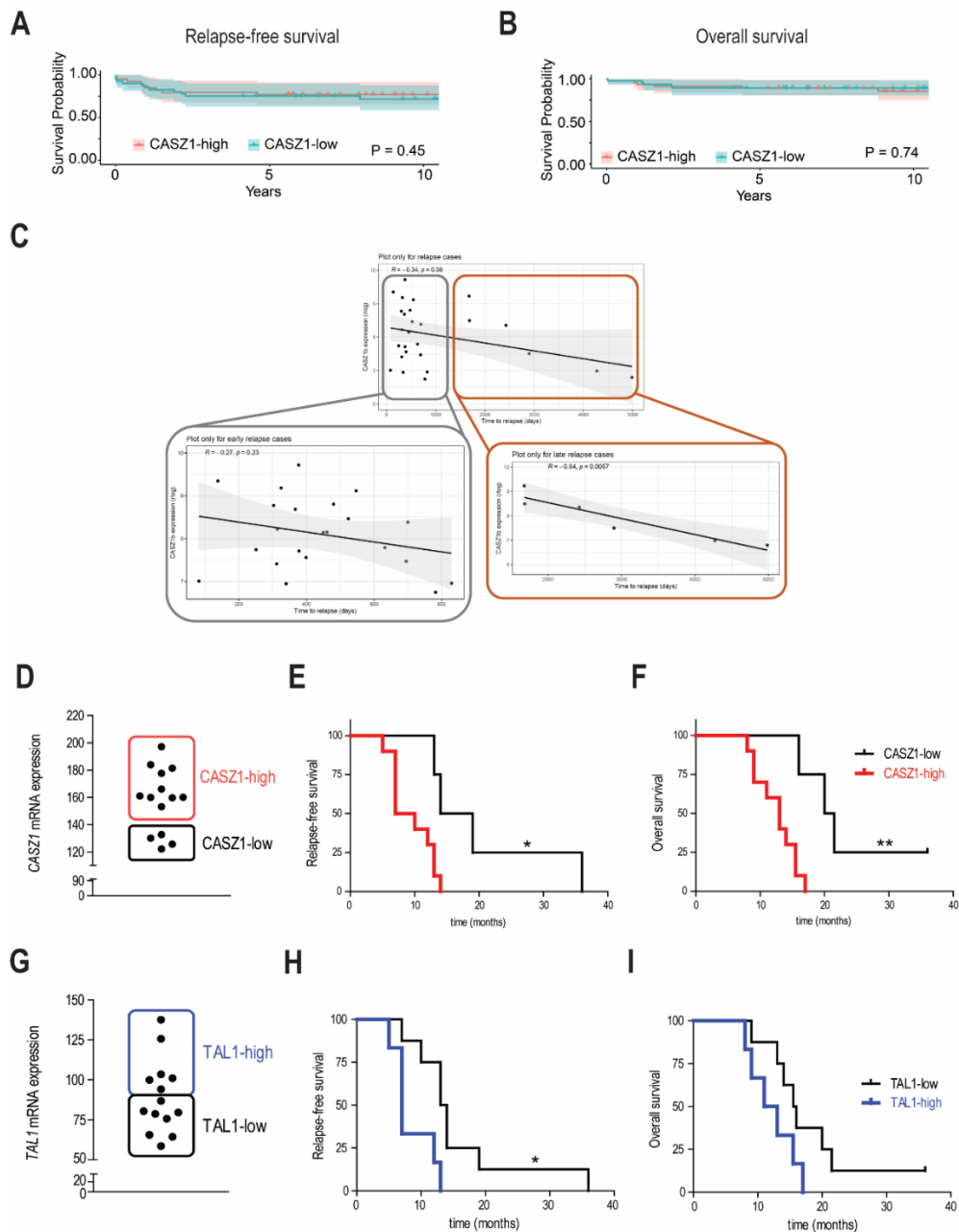
Supplementary Figure 9. PI3K inhibition dampens CASZ1-mediated effects in Ba/F3 cells. (A) Ba/F3-CASZ1 cells were cultured for 24h in the presence of 25 μ M LY294002 (PI3K inhibitor) or vehicle (DMSO). The cells were lysed and PI3K signaling activation was evaluated by immunoblot analysis of AKT and GSK3 β phosphorylation levels of p27^{Kip1} total levels. Lamin B was used as loading control. The data are representative of two independent experiments. (B-C) Ba/F3-CASZ1 cells were cultured in the presence of 25 μ M LY294002 (PI3K inhibitor) or vehicle (DMSO) for the indicated time points. Viability (B) and proliferation (C) were determined at the indicated time points. (B-C) The values represent the mean \pm standard deviation of at least three experiments. * $p < 0.05$; *** $p < 0.001$, one-way analysis of variance.



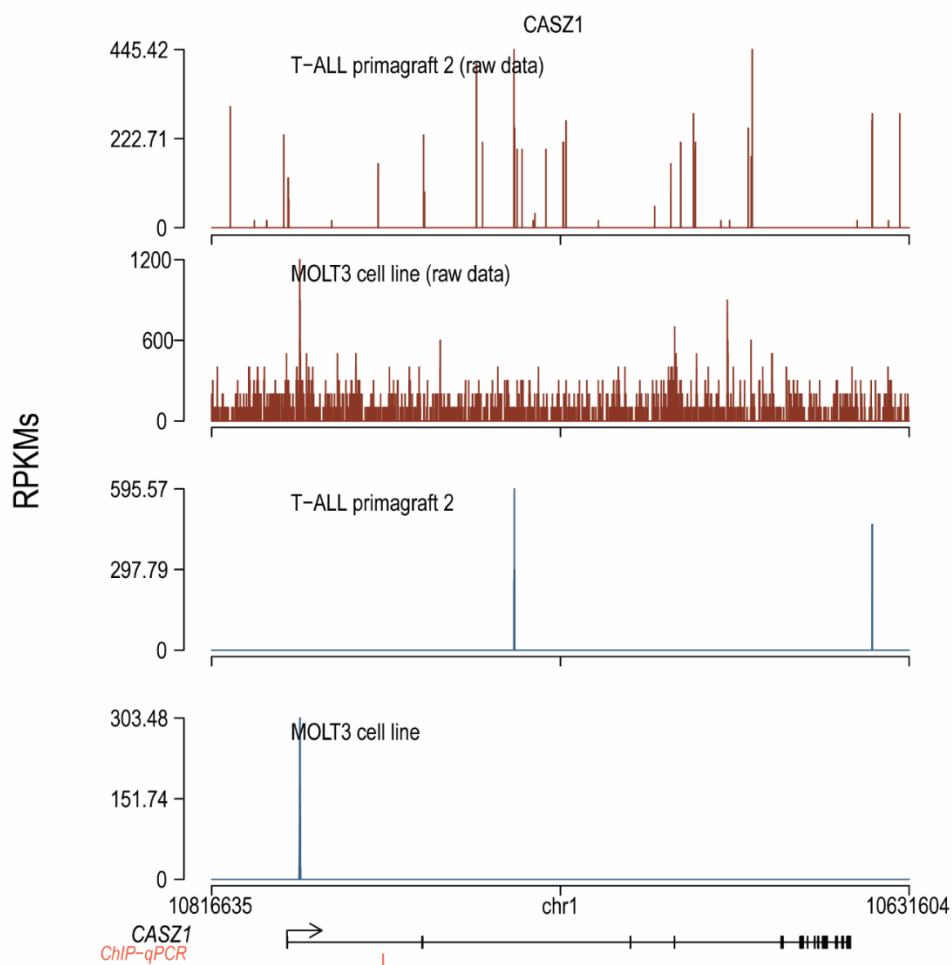
Supplementary Figure 10. Decreased *CASZ1* expression reduces T-ALL cellular viability and proliferation. (A-C) Jurkat cells were nucleofected with siRNA targeting *CASZ1* and cultured for 48h. (A) *CASZ1b* transcript levels were detected by qPCR and the values were normalized to the control condition (siRNA CTRL). (B) Viability levels and (C) proliferation was determined as described in the material and methods section. Values represent the mean \pm standard deviation of experimental triplicates of a representative experiment (n=3). * $p < 0.05$.



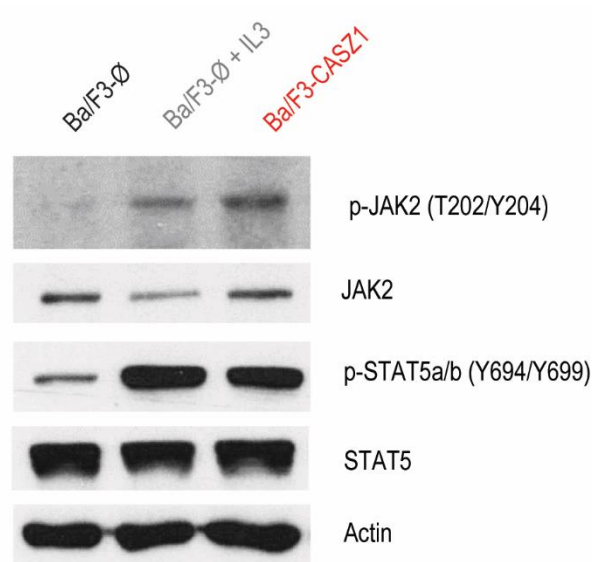
Supplementary Figure 11. CASZ1 overexpression in T-ALL has no impact on cell viability or proliferation under non-stress conditions. The indicated T-ALL cell lines stably expressing *CASZ1b* or mock vector were analyzed for (A) *CASZ1* mRNA levels, determined by qPCR and normalized to the transcript levels of the *18S* house-keeping gene. The same cell lines were cultured in complete medium (RPMI-10) and viability (B) and proliferation (C) were determined at the indicated time points. (A-C) The values indicated represent the mean \pm standard deviation of at least three experiments. ** $p < 0.01$; *** $p < 0.001$, student's t-test.



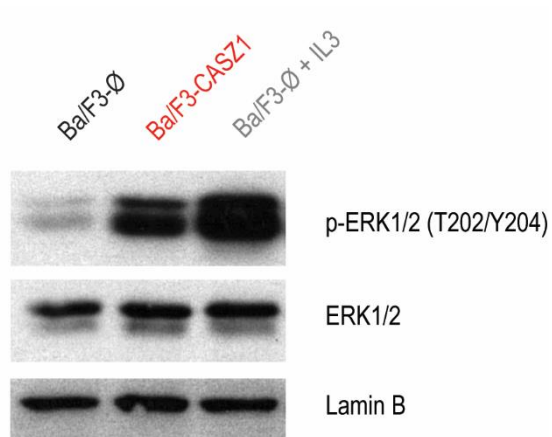
Supplementary Figure 12. CASZ1 expression in T-ALL associates with poor prognosis. (A-B) Relapse-free (A) and overall (B) survival in Total 15 and 16 cohorts (n=153) treated at St. Jude Children’s Research Hospital. T-ALL patients with CASZ1-high (top 46 cases; 30%; red) and CASZ1-low (bottom 46 cases; 30%; blue) were compared and plotted in Kaplan-Meier curves with confidence interval. (C) Correlation coefficients between CASZ1 expression and time to relapse for total relapse, early relapse and late relapse cases with the St. Jude’s patient cohort shown in (A-B). (D) CASZ1 expression was determined in the publicly available GSE18497 dataset, as described in the material and methods section, and cases separated into CASZ1-high (n=10, expression above 140) and CASZ1-low (n=4, expression below 140). (E,F) Kaplan-Meier curves of (E) relapse-free and (F) overall survival of CASZ1-high versus CASZ1-low T-ALL patients, as defined in (D). (G) TAL1 expression was determined in the GSE18497 dataset and cases separated into TAL1-high (n=6, expression above 94) and TAL1-low (n=8, expression below 94). (H,I) Kaplan-Meier curves of (H) relapse-free and (I) overall survival of TAL1-high versus TAL1-low T-ALL patients, as defined in (G). * p<0.05; ** p<0.01; *** p<0.001, Log-rank (Mantel-Cox) test.



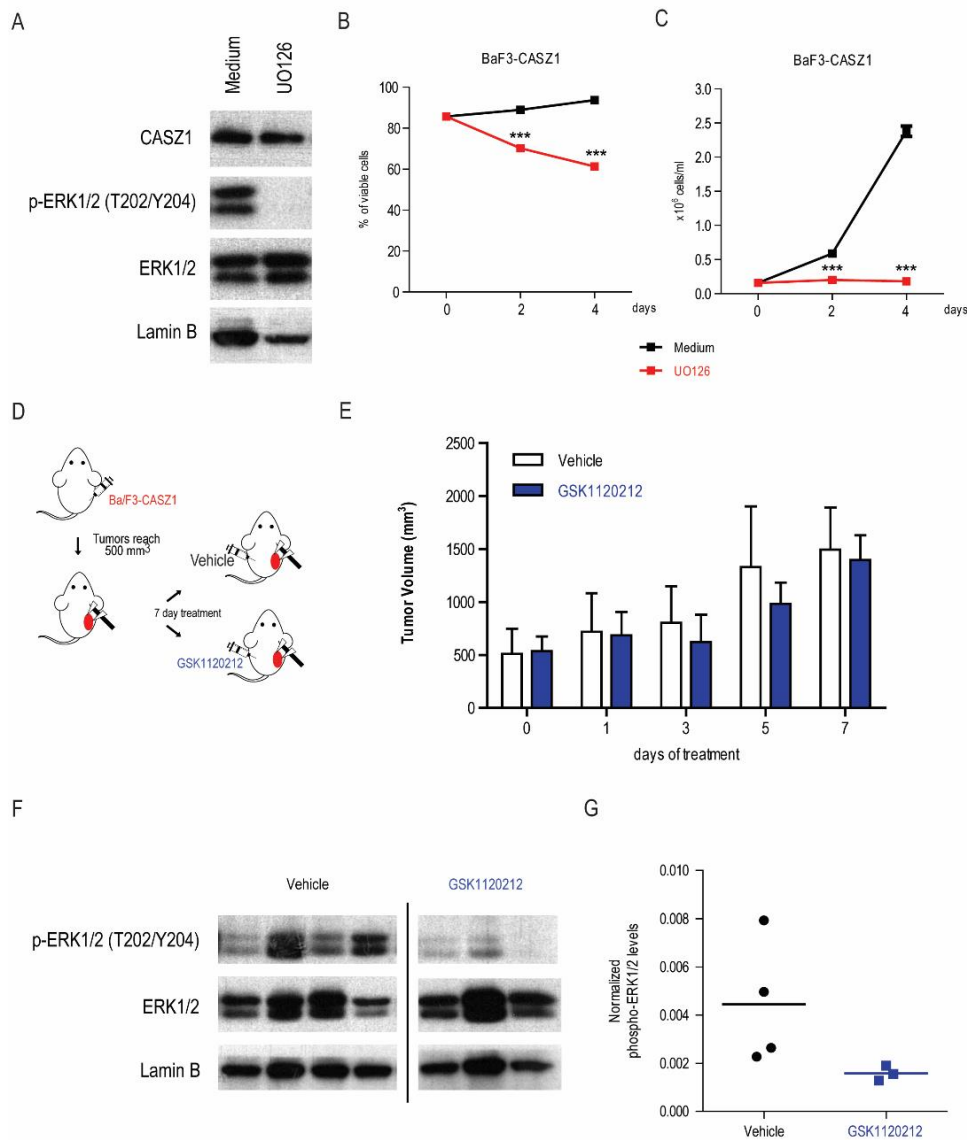
Supplementary Figure 13. ChIP-seq signals of TAL1 at the genomic loci of *CASZ1* in MOLT3 cells (GSE59657) and a T-ALL primagraft (GSE29181). ChIP-seq signals are represented as reads per kilobase per million mapped reads (RPKMs) of the raw coverage (top profiles in red) or the significantly enriched regions (bottom profiles in blue). The genomic region assessed by ChIP-qPCR is highlighted in red.



Supplementary Figure 14. CASZ1 expression activates JAK-STAT signaling pathway. Ba/F3-Ø and Ba/F3-CASZ1 cells were cultured in medium alone. Ba/F3-Ø were cultured in IL-3 as positive control. JAK-STAT signaling pathway activation was evaluated by immunoblot detection of the phosphorylation levels of JAK2 and STAT5A/B in the indicated residues. Total levels of JAK2 and STAT5A/B were also analyzed and Actin was used as loading control. Data are representative of two independent experiments.



Supplementary Figure 15. *CASZ1* expression activates MEK-ERK signaling pathway. Ba/F3-Ø and Ba/F3-CASZ1 cells were cultured in medium alone. Ba/F3-Ø were cultured in IL-3 as positive control. MEK-ERK signaling activation was evaluated by immunoblot detection of the phosphorylation levels of ERK1/2 in the indicated residues and Lamin B was used as loading control. Data are representative of two independent experiments.



Supplementary Figure 16. MEK-ERK signaling pathway activation is dispensable for CASZ1-induced expansion of Ba/F3 cells *in vivo*. (A) Ba/F3-CASZ1 cells were cultured for 24h in the presence of 50 μ M UO126 (MEK1/2 inhibitor) or vehicle (DMSO; indicated as Medium). Cells were lysed and MEK-ERK signaling activation was analyzed by detecting the phosphorylation levels of ERK1/2 in the indicated residues by immunoblot. Lamin B was used as loading control. Data are representative of two independent experiments. (B,C) Ba/F3-CASZ1 cells were cultured in the presence of 50 μ M UO126 or vehicle (DMSO; indicated as Medium) for the indicated time points. Viability (B) and proliferation (C) were determined in the indicated time points as described in the material and methods of the manuscript. (D-G) 8 week old NSG mice were injected subcutaneously with 10⁷ Ba/F3-CASZ1 cells. Once the tumors reached 500mm³, mice were randomized to receive either the clinical-grade MEK1/2 inhibitor Trametinib/GSK1120212 (n=5) or vehicle (n=5) for seven consecutive days. (D) Schematic representation of the experimental layout. (E) Longitudinal analysis of tumor growth upon treatment initiation. (F) Vehicle- or GSK1120212-treated tumors were collected, and phosphorylation and total levels of ERK1/2 assessed by immunoblot analysis. Lamin B was used as loading control. (G) ERK1/2 phosphorylation levels in (F) were measured by densitometry analysis, and then normalized to total ERK1/2 and Lamin B levels.

Supplementary Table 1. Quantitative PCR primer sequences.

Gene	Forward primer 5'→ 3'	Reverse primer 5' → 3'
<i>ALDH1A2</i>	AGGAGATCTTTGGCCCTGTT	TCTGGGCATTTAAGGCATTGTAAC
<i>CASZ1a</i>	CAGGCTAGGTTGCAAGTACA	CTCATCTGTCTCAGCATCCA
<i>CASZ1b</i>	AGAAGTGAGTCCCTCGATGA	AGCATCTTTGGCTAGAAGGA
<i>CASZ1 (OE)</i>	TTCCACCATACCCCAGATGC	GGACTCACTTCTCCTGGAAGT
<i>GAPDH</i>	GGAGTCAACGGATTTGGTTCG	GACAAGCTTCCCCTTCTCAG
<i>TAL1</i>	ATTACTGATGGTCCCCACAC	GGAGGATCTCATTCTTGCTG
<i>zβ actin</i>	GCTGTTTTCCCCTCCATTGTT	TCCCATGCCAACCATCACT
<i>zCD4</i>	TCTTGCTTGTTCATTCCGC	TCCCTTTGGCTGTTTGTATTGT
<i>zCD8</i>	CGAAAAAGGAGCAAAGCCCAT	ATGGTGGGGACATCGTCTTG
<i>zCD37</i>	GTCAGTGGGGAAAGAAACGGA	TTCCAACCACAGCATTCTTCT
<i>zCD79a</i>	ATGCCATTGCTGGTCTTCA	CCCTCGCTGAGGTTCAAAGT
<i>zIGM</i>	CCGAATACAGTGCCACAAGC	TCTCCCTGCTATCTTTCCGC
<i>zLCK</i>	GCCGAAGAAGATCTCGATGGT	TCCCATGTTTACGTATTTTGTGCG
<i>zPAX5</i>	AAGGCAGTTACTCCACACCC	ACCGTACTCCTGCTGAAACAC
<i>zRAG2</i>	TGAGACTCAGAAGCGCATGG	ACCAAGTACGACTGTGGCTG
<i>zTCRα</i>	CTTAAACGTCGGCTGTCCG	TGAACAAACGCCTGTCTCCT
<i>zTCRβ</i>	AGTTGCAGGTGGATATGACCG	ATGACAAGGCCATACAGTCCG
<i>18S</i>	GGAGAGGGAGCCTGAGAAACG	CGCGGCTGCTGGCACCAGACTT

LEGEND TO SUPPLEMENTARY TABLE 2

Supplementary Table 2 (in excel file). RNA sequencing gene list in CASZ1-overexpressing versus mock-transduced Ba/F3 cells. Columns correspond, from left to right, to Ensembl ID, Gene name, log₂-transformed fold change (log₂FC), and adjusted P-value (adj. P-value).